

Vortex stretching in a laminar boundary layer flow

P. Petitjeans, J. E. Wesfreid, J. C. Attiach

351

Abstract A new technique to produce controlled stretched vortices is presented. The initial vorticity comes from a laminar boundary layer flow and the stretching is parallel to the initial vorticity. This low velocity flow enables direct observations of the formation and destabilization of vortices. Visualizations are combined with quasi-instantaneous measurements of a full velocity profile obtained with an ultrasonic pulsed Doppler velocimeter. Several modes of destabilization are observed and include pairing of two vortices, hairpin deformation, and vortex breakdown into a coil shape.

1

Introduction

It is of great fundamental interest to understand the formation and dynamics of filamentary vortices with intense vorticity in turbulent flows. It has been shown numerically by Siggia (1981) that the regions of largest vorticity concentration in a turbulent flow look like filaments. Filaments have been observed in experiments by Cadot et al. (1995) in a turbulent flow in a cylinder between two counter-rotating stirrers. The observed filaments have been shown to correspond to low pressure regions. They are generated by local stretching of the vorticity sheets (Neu 1984). The topic of vortex stretching is indeed interesting and relevant for a better understanding of fundamental mechanics in turbulence.

This note presents a new experimental set-up to study the effects of stretching on a controlled vorticity sheet coming from a laminar boundary layer flow on a flat plate. This flow is not turbulent. Therefore, the characteristic time and length scales are large enough to enable study of the instability. First observations illustrating the capabilities of this experiment are presented. Thus, this experiment opens the possibility to accomplish quantitative measurements of the dispersion relation of vortex instabilities.

2

Experiments and observations

The experimental set-up is a low-velocity water channel constructed of plexiglass with well controlled flow. The flow is generated by a constant head pressure tank. A diffuser keeps the flow laminar with a minimum of perturbation. The key elements of the channel are presented in Fig. 1. In this straight part (40 cm × 12 cm × 5 cm) the flow develops laminar boundary layers with a velocity of order 1 cm/s far away from the wall. The Reynolds number based on the boundary layer thickness is $Re_\delta \approx 100$. The boundary layers on the lower and upper walls form the initial vorticity, $\omega = \pm \omega z$. A flow slot on each lateral wall (Fig. 1) is used to stretch the vorticity sheet parallel to the vorticity vector. The total flow rate through the channel is controlled as well as the flow rate in the flow slots; consequently, the initial vorticity can be controlled (via the thickness of the boundary layer) as well as the stretching. The formation of strong periodic vortices by roll-up of fluid sheets is obtained when the stretching is large enough. The formation, development and destabilization of these vortices is visualized by injection of a sheet of fluorescent dye (fluoresceine) on the wall, 2 cm upstream from the flow slots (Fig. 1). The dye is injected into the flow utilizing a thin transverse slot (1 mm thick and is inclined at 30° with respect to the bottom). An argon laser beam, expanded by passing through two mutually perpendicular cylindrical lenses, is used to fluoresce the dye, permitting the visualization of the formation of the rolls (Fig. 1). The dye sheet separates from the injector, and penetrates into the vortex by winding around the axis. Because of a low molecular diffusion coefficient ($D \approx 3.6 \times 10^{-6}$ cm²/s), it is possible to distinguish several layers of dye (≈ 50) turning around the core of the vortex in a helical way until the dye arrives at the core. A very thin dye filament is observed that shows the core of the vortex. In the core, the dye is removed to the two sides towards the slots in the lateral walls of the channel, which shows that the stretching velocity occurs only at the core of the vortex. Another vortex is then generated, and so on, with a periodicity due to the permanent longitudinal flow. Once a vortex is created, it is possible to study it in more detail by stopping the flow downstream, thereby producing a relatively stationary, permanent vortex.

In addition to the classical techniques of measuring the velocity such as laser Doppler anemometry and PIV, the fully quasi-instantaneous vertical velocity profile, $v(y)$, is obtained with an ultrasonic Doppler velocimeter DOP 1000. The DOP 1000¹ is an Ultrasonic Pulsed Doppler Multigate Velocimeter

Received: 3 April 1996/Accepted: 4 October 1996

P. Petitjeans, J. E. Wesfreid
Laboratoire de Physique et de Mécanique des Milieux Hétérogènes
URA CNRS 857
Ecole Supérieure de Physique et de Chimie Industrielles (ESPCI)
10, rue Vauquelin, F-75005 Paris, France

J. C. Attiach
Lot Oriol, 9 avenue de Laponie, F-91951 Les Ulis Cedex, France

Correspondence to: P. Petitjeans

¹ by Signal Processing S. A.

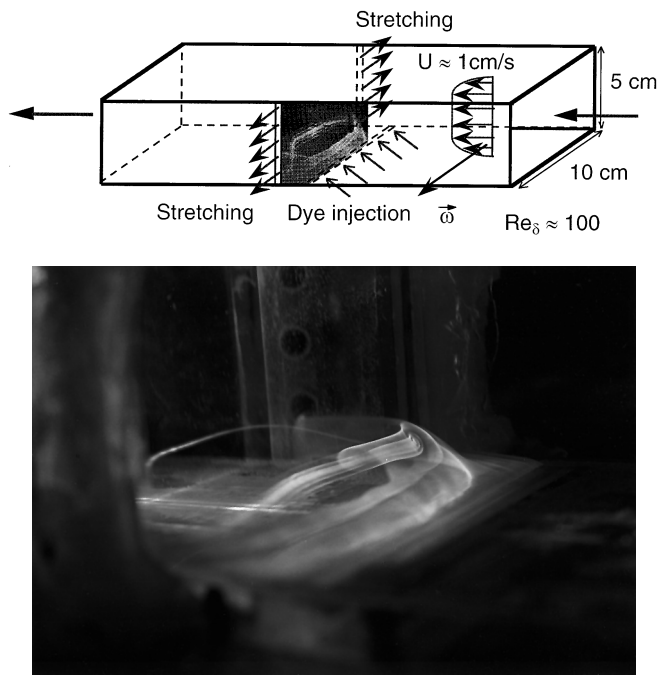


Fig. 1. The straight part of the experimental set-up where vortices are created with stretching by means of the slots on the sides. Visualization of the formation of a vortex (flow goes from right to left) shows how the dye sheet penetrates into the vortex by winding around the axis

that measures a velocity component profile along the transducer axis. The transducer generates a pulse wave that propagates as a thin acoustic beam, representing the global measurement volume. The maximum measurement depth, P_{\max} , is determined by the repetition frequency of the pulses (f_{PRF}) which has the relation, $P_{\max} = c/(2 \cdot f_{\text{PRF}})$. The typical value of f_{PRF} used in the experiment is 976 Hz. This gives a P_{\max} value of 77 cm. This depth can be divided by 2, 4 or 8 to increase the spatial resolution. Assuming that the sound speed, c , in the medium is constant (1500 m/s in water), the time delay between two pulses represents both the outgoing and the incoming distance covered by the pulse wave. Every particle of suitable diameter going across this beam will produce an echo collected by the transducer (one transducer is used in backscatter mode), and analyzed by the multigate processor of the DOP 1000. Two measurements are extracted from the echo signal: the Doppler frequency (to obtain the probe-axis component of the velocity), and the time delay between the emission of the pulse and the subsequent echo (to obtain the position along the transducer axis). A maximum of 114 positions along the measurement range are obtained. It is possible to build velocity profiles using between 16 and 512 pulses. This gives a time step range between two full profiles of 0.03 and 1.05 s, respectively. The probe is placed vertically at the top of the channel and measures the velocity profile, $v_i(y)$, across the wall as a function of time. In this experiment, the time step between two profiles of 114 points is $\Delta T = 0.12$ s. This produces a $v(y, t)$ dataset that can be visualized using analysis software² which builds an image where the velocities are linearly scaled between 0 and 255 (in grayscale). The data is

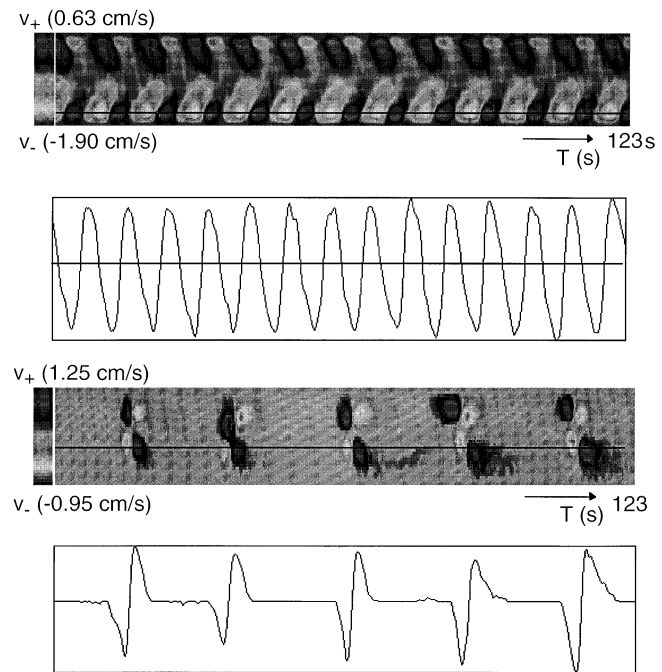


Fig. 2. Shown are two examples of the vertical velocity as a function of time from 0 to 123 s. A slice along the black line in of these images gives the evolution of the vertical velocity with time at the position where the centers of the vortices are located

processed with a median image filter for noise reduction. The advantage of using this filter on the image instead of on the initial data, is that the filter reduces noise by taking into account both velocities forward and backward in time as well as space. Two examples of what is obtained are shown in Fig. 2, with observations of a double array of vortices on the upper and lower walls. Only the lower array is visualized by the dye since it is injected only on the lower wall, but it is clear that there is an equivalent vorticity sheet on the upper wall, which is also stretched due to the slots constituting the full height of the lateral walls (Fig. 1). The vorticity in the array of vortices on the lower wall is larger than that on the upper wall because of the injection of dye on this wall, which enhances the initial shear. The vortices are emitted regularly. Vortices on the upper wall and vortices on the lower wall are emitted in phase and probably interact in a way that the authors have not studied yet. Vortices are then advected by the flow. Because of the boundary layer profile, the flow closer to the wall produces a lower advection velocity of a vortex. To the contrary, the flow far away from the walls has a larger velocity, so that the part of a vortex in this region is advected faster, which in combination with the slow moving part, produces this deformation and inclines the roll. This mechanism is also responsible for the vortex pairing instability (Saffman and Baker 1979) that is observed clearly in this experiment. A perturbation of the fastest moving part of a vortex (farthest from the wall) catches

² NIH Image freeware software, from the National Inst. of Health, available via ftp at zippy.nimh.nih.gov

up with the slowest moving part of the preceding vortex. The two vortices first rotate around each other, and then coalesce into a stronger vortex. This instability can be controlled by means of the advection velocity.

Another observed instability concerns the deformation of the vortex. A transversal perturbation toward the center of the channel deforms the vortex line and eventually produces a localized longitudinal line (hairpin). This effect is magnified by the attachment of the vortex to the slots on the walls.

The last instability observed is a “vortex breakdown” instability (Hall 1972). It normally happens when a type of solitary wave propagates along the vortex producing a loss of its axial symmetry. The vortex deforms in a helical fashion and collapses into a “coil shape” as a turbulent spot. This transition is clearly observed in this experiment and gives a picture of some intermittent features of turbulent flows.

3

Conclusion

At this stage, the main point of this work is the design of an experimental set-up which enables direct observation of the dynamics of vortices under stretching, and gives direct access to the fundamental mechanisms which play a role in this problem. Several forms of destabilization are observed; including vortex pairing, sinuous vortex deformation, and vortex breakdown. Details of the intermittent “coil shape” transition are seen as the ultimate evolution of vortex break-

down. Velocity profiles deform the vortex in an elliptical manner. As it is known from the inviscid theory of stability, elliptical vortices can produce three-dimensional instabilities similar to what is observed in these experiments.

The practice of using ultrasound anemometry to measure the velocity of flow is not new. Nevertheless, the apparatus that is used allows for very simple acquisition of velocity profiles (along the axis of the probe) at rates related to the characteristic time of the moderate Reynolds number used in these experiments. This measurement, combined with flow visualization, has allowed insight to the fundamental mechanisms that define the generation and the dynamics of stretched vortices. In order to systematically study the stability of these structures, work is in progress using a new facility, which is fully devoted to take advantage of this new technique of vortex stretching.

References

- Cadot O; Douady S; Couder Y** (1995) Characterization of the low pressure filaments in three-dimensional turbulent shear flow. *Phys Fluids* 7: 630–646
- Hall MG** (1972) Vortex breakdown. *Ann Rev Fluid Mech* 4: 195–218
- Neu JC** (1984) The dynamics of stretched vortices. *J Fluid Mech* 143: 253–276
- Saffman PG; Baker GR** (1979) Vortex interactions. *Ann Rev Fluid Mech* 11: 95–122
- Siggia ED** (1981) Numerical study of small-scale intermittency in three-dimensional turbulence. *J Fluids Mech* 107: 375